Bioconjugate Chemistry

Article

pubs.acs.org/bc

Dual-Purpose Linker for Alpha Helix Stabilization and Imaging Agent Conjugation to Glucagon-Like Peptide-1 Receptor Ligands

Liang Zhang,[†] Tejas Navaratna,[†] Jianshan Liao,[†] and Greg M. Thurber*[,†,‡]

[†]Department of Chemical Engineering, [‡]Department of Biomedical Engineering, University of Michigan, Ann Arbor, Michigan 48109, United States

Supporting Information

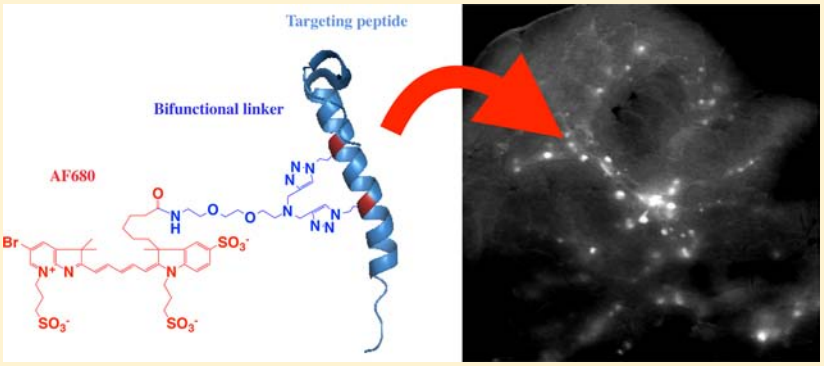

ABSTRACT: Peptides display many characteristics of efficient imaging agents such as rapid targeting, fast background clearance, and low non-specific cellular uptake. However, poor stability, low affinity, and loss of binding after labeling often preclude their use *in vivo*. Using glucagon-like peptide-1 receptor (GLP-1R) ligands exendin and GLP-1 as a model system, we designed a novel α-helix-stabilizing linker to simultaneously address these limitations. The stabilized and labeled peptides showed an increase in helicity, improved protease resistance, negligible loss or an improvement in binding affinity, and excellent *in vivo* targeting. The ease of incorporating azidohomoalanine in peptides and efficient reaction with the dialkyne linker enable this technique to potentially be used as a general method for labeling α helices. This strategy should be useful for imaging beta cells in diabetes research and in developing and testing other peptide targeting agents.

INTRODUCTION

The ability to image and observe cellular phenomena both *in vivo* and *in vitro* plays a crucial role in understanding disease progression and treatment response.[1,2] Molecular imaging agents enable investigators to probe the dynamics of specific biologic interactions under normal and pathological conditions. In principle, peptides are ideal imaging agents due to their low molecular weight,[3] rapid clearance from background tissues, and ability to mimic protein−protein interactions for high binding specificity.[4] However, these agents suffer from several problems, including poor protease stability, low affinity from lack of a stable conformation, and difficulty in labeling with fluorescent and/or radioactive probes without disrupting binding.[5] Due to recent advances in synthesis techniques, there is renewed interest in using stabilized α helices with improved protease resistance and binding affinity for targeting both intracellular[6,7] and extracellular[8] proteins. Side chain cross-linking reactions to promote an α-helix conformation include olefin metathesis,[9] copper catalyzed azide−alkyne reactions,[10,11] lactam ring formation,[12] and disulfide bond formation,[13,14] among others.[8]

In many cases, stabilizing the α helix increases helicity, improves binding affinity, and/or increases protease resistance.[15] However, this is not universally true since the introduction of the side chain cross-linker introduces two mutations into the sequence and along with the linker itself, these can change intra- and intermolecular interactions.[16−18] The sequence mutations and cross-linker can impart both positive and negative contributions to the free energy of helix formation and free energy of binding, making the net impact challenging to predict *a priori* from structural considerations alone. Typically biophysical characterization is necessary to test the overall effect, which we have done for the agents presented here.

In the context of imaging agent development, while these stabilizing structures have the potential to improve protease stability and binding affinity by locking molecules in a helical conformation, this exacerbates the problem of labeling the peptide since multiple modifications must now be done without disrupting the binding interface. To address this issue, we synthesized probes using a novel linker (Figure 1A) to simultaneously label and stabilize an α helix to improve

Received: December 10, 2014
Revised: January 13, 2015
Published: January 16, 2015

DOI: 10.1021/bc500584t
Bioconjugate Chem. 2015, 26, 329−337

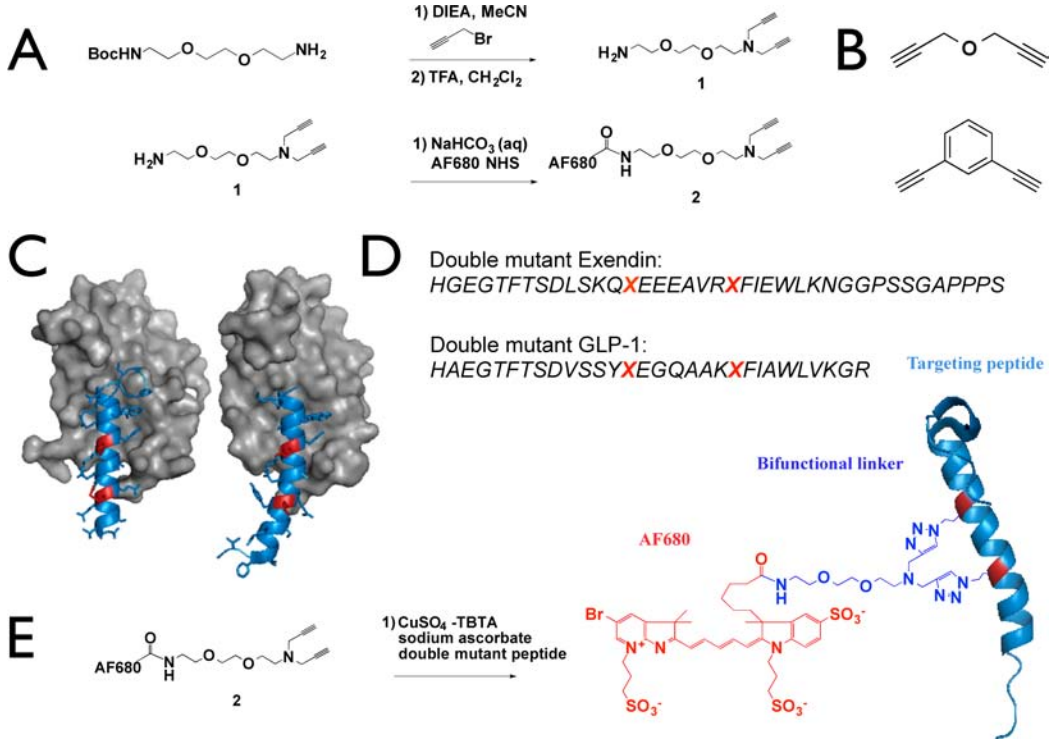

Figure 1. Linker design and synthesis. A Boc-protected hydrophilic spacer was alkylated with propargyl bromide and deprotected to provide a free amine for fluorophore conjugation (A). Propargyl ether (top) and 1,3-diethynylbenzene (bottom) were used to test steric effects of the dye and rigidity of the linker (B). The crystal structure of exendin (left, PDB 3C59) and GLP-1 (right, PDB 3IOL) are shown with the modified residues highlighted in red (C) and the double mutant sequences (D). The peptides were reacted with the linker to form labeled and stabilized α helices (E).

protease stability while maintaining *in vitro* and *in vivo* binding affinity. This was compared with two non-fluorescent stabilizing linkers (Figure 1B) to separate the impact of the fluorophore from helix stabilization.

One promising application of targeting peptides is to utilize modified glucagon-like peptide-1 receptor (GLP-1R) binding peptides for imaging beta cells in diabetes.[19,20] Beta cells express moderate-to-high levels of GLP-1R, resulting in excellent target specificity versus exocrine cells within the pancreas. These properties have led several investigators to explore the use of radiolabeled exendin molecules for tracking beta cell mass in diabetes.[19−25] However, the molecular properties of the radiolabeled peptide require further optimization before obtaining clinical utility.[23,25] Using a novel dialkyne linker with a functional handle for attaching an imaging agent, we synthesized a dual-purpose linker to simultaneously stabilize and label α helices. Here, we demonstrate improved protease resistance and *in vivo* targeting of these stabilized GLP-1R ligands for visualizing the beta cell mass in the pancreas.

Ligands GLP-1 and exendin share significant homology and bind to the same pocket on GLP-1R, but they exhibit distinct differences. Exendin binds in a straight α-helix conformation, whereas GLP-1 has a small kink around glycine-22[26] (Figure 1C). Exendin also has significant helical structure in solution, whereas GLP-1 is almost completely disordered.[27] This allowed us to investigate several aspects of the linker, including the impact on helicity, flexibility, affinity, and stability.

One turn of an α helix constitutes approximately 3.6 amino acid residues. As a result, i, i + 4 and i, i + 7 are frequent candidates for cross-linking residues between either one or two adjacent loops.[12] To generate a staple across two loops, we postulated that non-natural azide-containing amino acids could be introduced and cross-linked at i, i + 7 residues in exendin-4 and GLP-1 through incorporation of azidohomoalanine (AHA) during solid-phase peptide synthesis (SPPS). A novel dialkyne linker is used to bridge the two AHA side chains and stabilize the helix while introducing a functional handle for labeling. The chemistry utilizes the well-studied copper-catalyzed azide−alkyne cycloaddition (CuAAC) for high-yielding and specific cross-linking of the desired residues.

The AHA substitution locations were selected using crystal structures[26,28] for the receptor−ligand interaction as well as alanine scan data of GLP-1 with sequence alignment for exendin-4.[29] Previous work labeling exendin with fluorescent tags has shown variable tolerance (negligible impact to >30-fold reduction in binding) at several positions with different fluorophores along the peptide backbone.[30] The requirements for a stabilizing linker are even more stringent. First, the linker must be located within the α-helix portion of the peptide, ruling out labeling of the C- and N-terminal regions. Second, the cross-link necessitates a larger structure adjacent to the peptide compared to a single fluorophore. Ultimately, methionine at the 14th position (M14) and leucine at the 21st (L21) were substituted with AHA for exendin-4 (Figure 1C,D) to generate double mutant exendin. Similarly, L20 and E27 substitutions were made to GLP-1 (7−36) for double mutant GLP-1. We present novel stabilized GLP-1R ligands cross-linked with dialkyne linkers (Figure 1E) of varying rigidity and demonstrate that all conjugates maintain GLP-1R-specific targeting. To abbreviate the structure names, the stabilized α helices of exendin generated with the AlexaFluor 680 linker, propargyl ether, and 1,3-diethynylbenzene are named AF680 sExendin, PropE sExendin, and DEB sExendin, respectively. AlexaFluor

DOI: 10.1021/bc500584t
Bioconjugate Chem. 2015, 26, 329−337

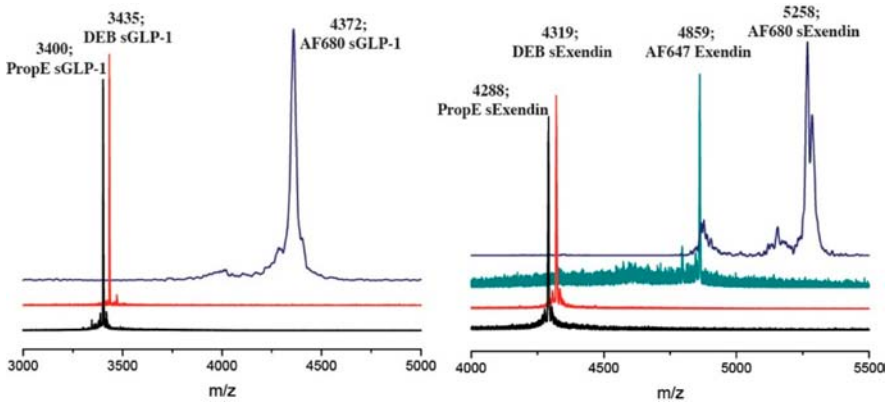

Figure 2. MALDI-TOF mass spectrometry traces of purified peptides showing the successful synthesis of stabilized GLP-1 and exendin helices.

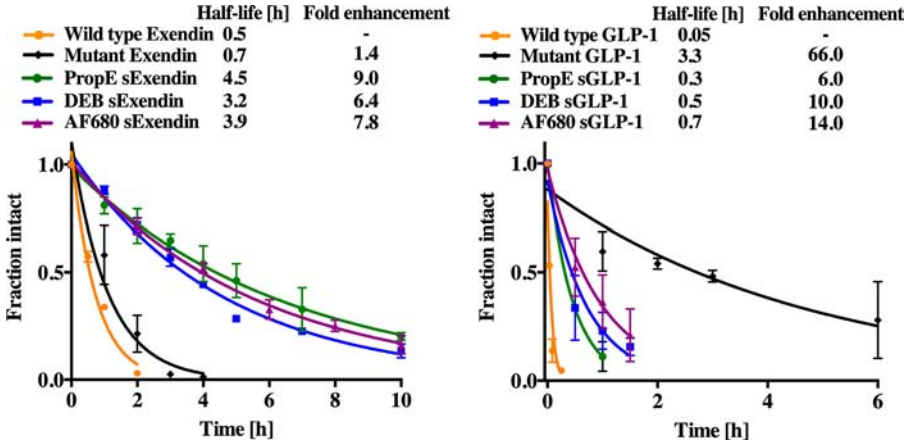

Figure 3. Protease stability of stabilized peptides. Digests were run on HPLC and monitored at 254 nm to separate intact versus degraded fragments, and areas were fit to an exponential decay.

680 linker, propargyl ether, and 1,3-diethynylbenzene stabilized GLP-1 are named AF680 sGLP-1, PropE sGLP-1, and DEB sGLP-1, respectively. The novel structures should prove to be useful for developing stabilized α-helix imaging agents.

RESULTS

Stabilized α-helical imaging peptides were generated using a novel dialkyne linker as shown in Figure 1A. To generate the dual-purpose linker, N-Boc-2,2′-(ethylenedioxy)diethylamine was alkylated with excess propargyl bromide, followed by deprotection with trifluoroacetic acid and subsequent purification via flash chromatography. The resulting intermediate **1** (Figure 1) was further purified on HPLC followed by conjugation to AF680 NHS ester to yield **2**.

GLP-1R ligands exendin-4 and GLP-1 were chosen to demonstrate the ability of the dual-purpose linker to simultaneously stabilize and fluorescently tag targeting peptides under investigation for imaging in diabetes.[20,21,30] On the basis of crystallography data for the receptor−ligand interaction, the M14 and L21 residues in exendin and L20 and E27 residues of GLP-1 were substituted with azidohomoalanine (Figure 1B, C). The *i*, *i* + 7 residues on exendin-4 and GLP-1 double mutant peptides were then reacted with **2** to stabilize and label the agents (Figure 1D). In addition to α-helix stabilization with **2**, we also investigated the effect of linker rigidity on the stabilized peptide with propargyl ether and the more rigid cross-linker 1,3-diethynylbenzene on the *i*, *i* + 7 residues of the GLP-1R ligands. A nonstabilized single mutant exendin-4 labeled with AF647 was synthesized for quantifying the binding affinity of propargyl ether and 1,3-diethynylbenzene stabilized peptides in competition assays. Both AF647−exendin and stabilized peptides were purified using HPLC and characterized by MALDI-TOF (Figure 2). MALDI for AF647 conjugated peptides, propargyl ether, and 1,3-diethynylbenzene stabilized peptides were collected using reflectron positive mode; fluorescently stabilized peptide MALDI spectra did not show up in reflectron positive mode and were collected using linear positive mode.

To determine the effect of the α-helix stabilization on protease resistance, wild-type GLP-1, wild-type exendin, and both double mutant GLP-1R ligands with and without *i*, *i* + 7 cross-links were subject to 500 ng/μL trypsin digests at room temperature. All of the unstabilized (wild-type and double mutant) peptides degraded rapidly except for double mutant GLP-1. Exendin is known to be more resistant to protease degradation, and the wild-type peptide had a longer half-life than that of wild-type GLP-1 (0.5 h versus 0.05 h), as anticipated. Unstabilized double mutant exendin with M14X and L21X modifications also digested rapidly in the presence of trypsin (half-life of 0.7 h, Figure 3). Compared to the protease resistance of wild-type exendin, the stabilizing cross-linker improved protease resistance over 9-fold in the case of PropE sExendin (half-life of 4.5 h) and over 6-fold for DEB sExendin (half-life of 3.2 h). AF680 sExendin demonstrated an almost 8-fold increase (half-life of 3.9 h). Stabilization of wild-type GLP-1 increased protease stability by 6-, 10-, and 14-fold for PropE

DOI: 10.1021/bc500584t
Bioconjugate Chem. 2015, 26, 329−337

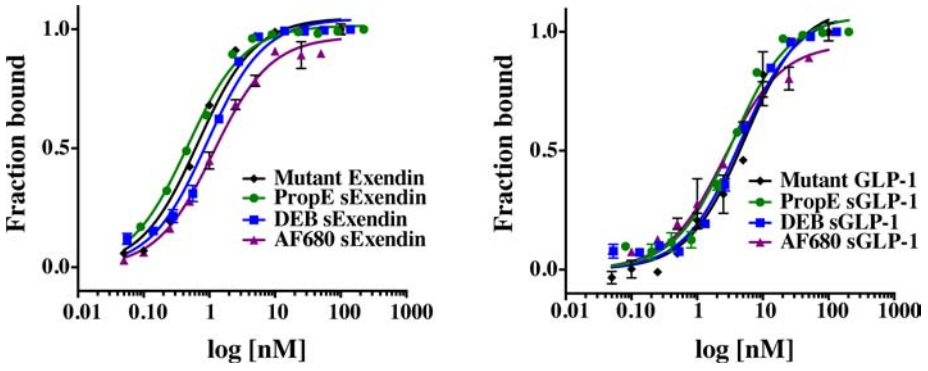

Figure 4. Representative affinity curves show negligible loss of affinity for exendin and a small improvement in binding for GLP-1 stabilized peptides.

sGLP-1, DEB sGLP-1, and AF680 sGLP-1, respectively. Surprisingly, double mutant GLP-1 had a very long half-life that was 1 to 2 orders of magnitude longer than that of wild-type GLP-1.

The stabilizing linker increased protease resistance relative to that for wild-type exendin and GLP-1, but the impact on binding affinity from the stabilizing linker was unknown. To test the influence on target binding, the affinity was measured in a binding assay using NIT-1 cells (Figure 4). Eleven- or twelve-point curves were done in triplicate for each experiment, and all experiments were repeated on 2−4 separate days. M14, L21 azidohomoalanine (AHA) substitutions in exendin-4 did not significantly lower the binding affinity, as anticipated by their orientation away from the binding pocket (Table 1). Similarly, GLP-1 also maintained high affinity despite the two substitutions. Stabilization of PropE sExendin and DEB sExendin yielded a K_d = 0.9 ± 0.7 nM and K_d = 0.8 ± 0.2 nM, respectively. The affinity was not statistically significantly different than that of the double mutant exendin (p = 0.6 compared to PropE sExendin, and p = 0.3 compared to DEB sExendin), demonstrating that steric hindrance from the linker did not significantly increase the K_d. AF680 sExendin had a K_d slightly above the original peptide but still maintained high affinity. For GLP-1, PropE sGLP-1 resulted in increased affinity with a K_d = 3.5 ± 0.8 nM. In the case of the more rigid DEB sGLP-1, α-helix stabilization resulted in similar affinity values. Stabilization with the new dual-purpose cross-linker in AF680 sGLP-1 also gave higher affinity for GLP-1R despite the presence of the fluorophore (K_d = 3.1 ± 0.7 nM). Both AF680 sGLP-1 and PropE sGLP-1 had statistically significantly higher affinity than that of double mutant GLP-1 (p = 0.04 for both), although DEB sGLP-1 did not (p = 0.08).

Table 1. Binding Affinity Values for Stabilized and Nonstabilized Exendin and GLP-1 Peptides

peptide	cross-linker	binding affinity (nM)
Exendin (M14X, L21X)	none	0.5 (±0.2)
Exendin (M14X, L21X)	propargyl ether	0.9 (±0.7)
Exendin (M14X, L21X)	1,3-diethynylbenzene	0.8 (±0.2)
Exendin (M14X, L21X)	AF680	1.4 (±0.3)
GLP-1 (L20, E27)	none	5.6 (±0.2)
GLP-1 (L20, E27)	propargyl ether	3.5 (±0.8)
GLP-1 (L20, E27)	1,3-diethynylbenzene	4.8 (±0.3)
GLP-1 (L20, E27)	AF680	3.1 (±0.7)

The increase in affinity for GLP-1 was unexpected given the typically negative impact of steric hindrance on K_d.[31] Helix stabilization is known to decrease the entropic penalty of binding by locking the peptide in an α helix and limiting the number of conformations,[8] although exceptions are known.[32] To investigate the effect of the dialkyne cross-linker on the helix structure, circular dichroism measurements were taken to determine the percent helicity (Figure 5). Nonstabilized double mutant exendin-4 displayed intermediate helicity (57%) in

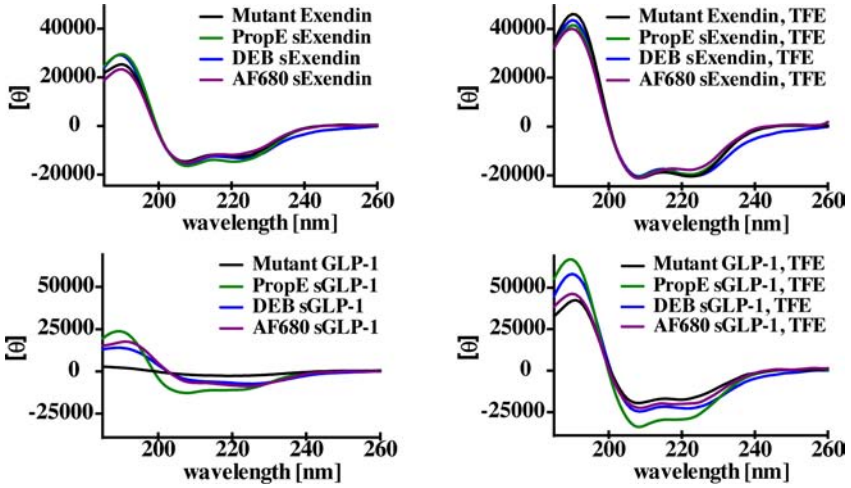

Figure 5. Stabilizing linker dramatically improves the helicity of GLP-1, with a smaller increase in helicity for the more highly structured exendin peptide.

DOI: 10.1021/bc500584t
Bioconjugate Chem. 2015, 26, 329−337

phosphate buffer (Table 2), consistent with the significant helicity of exendin.[27] The PropE sExendin and DEB sExendin had small increases in helicity (67 and 59%, respectively), and AF680 sExendin had 55% helicity. Calculations of the fractional helicity are based on estimates of the number of helical residues within the peptide sequence.[27] To experimentally validate these estimates, 50% trifluoroethanol (TFE) was used as a solvent to drive the peptides into a helical conformation. The highest values for exendin and GLP-1 derivatives were between 93 and 104%, indicating agreement between the literature estimate and experimental values reported here. All of the exendin peptides had elevated helicity in TFE (>80%). On the contrary, GLP-1 had very little helicity in phosphate buffer (7%), but stabilization with propargyl ether, 1,3-diethynylbenzene, and the AF680 stabilizing linker resulted in a significant increase in percent helicity (38, 23, and 30%). Higher helicity for stabilized peptides was maintained in 50% TFE buffer with 60% for the GLP-1 peptide and 104, 82, and 71% for PropE sGLP-1, DEB sGLP-1, and AF680 sGLP-1, respectively.

Table 2. Fractional Helicity for Stabilized and Nonstabilized Exendin and GLP-1 Peptides

peptide	cross-linker	χ^{helix}	χ^{helix} (TFE)
Exendin (M14X, L21X)	none	0.57	0.93
Exendin (M14X, L21X)	propargyl ether	0.67	0.9
Exendin (M14X, L21X)	1,3-diethynylbenzene	0.59	0.93
Exendin (M14X, L21X)	AF680	0.55	0.82
GLP-1 (L20, E27)	none	0.07	0.6
GLP-1 (L20, E27)	propargyl ether	0.38	1.04
GLP-1 (L20, E27)	1,3-diethynylbenzene	0.23	0.81
GLP-1 (L20, E27)	AF680	0.3	0.71

Owing to its higher stability, AF680 sExendin was used to demonstrate the *in vivo* imaging potential of the fluorescent helix stabilizing cross-linker. To show the specificity of the imaging agent for beta cells in the islets of Langerhans, AF680 sExendin was injected in C57BL/6 mice and allowed to circulate for 3 h. Blood samples were taken, and the half-life of AF680 sExendin in plasma was determined by fitting to a biexponential decay. We observed a fast decay $t_{1/2}$ of 2.7 min (91%) and a slow decay $t_{1/2}$ of 67 min (Figure 6). To confirm specific beta cell targeting, the animal was sacrificed after 3 h, and the pancreas removed. Macroscopic scans of the organ indicate AF680 sExendin signal in distinct, punctate spots spread along the pancreatic vasculature, indicating efficient targeting of the islets of Langerhans (Figure 6). A validated K12 labeled exendin peptide[21,33] is shown for comparison. The pancreas was then processed for histology, and islets were stained with an anti-insulin antibody (Figure 6). Colocalization between *in vivo* delivered AF680 sExendin and anti-insulin demonstrate specific targeting of islets *in vivo*.

DISCUSSION

Peptides possess many properties that are ideal for imaging agents.[34,35] Their low molecular weight allows rapid uptake in target tissue, fast clearance from background regions, and low non-specific uptake. Despite these advantages, significant challenges exist including poor stability, low affinity, and difficulty in labeling without lowering affinity due to steric hindrance of binding. To help address some of these issues, we designed a dual-purpose linker to simultaneously label an α-helix peptide while stabilizing the secondary structure. Because not all stabilized helices exhibit improved properties, we

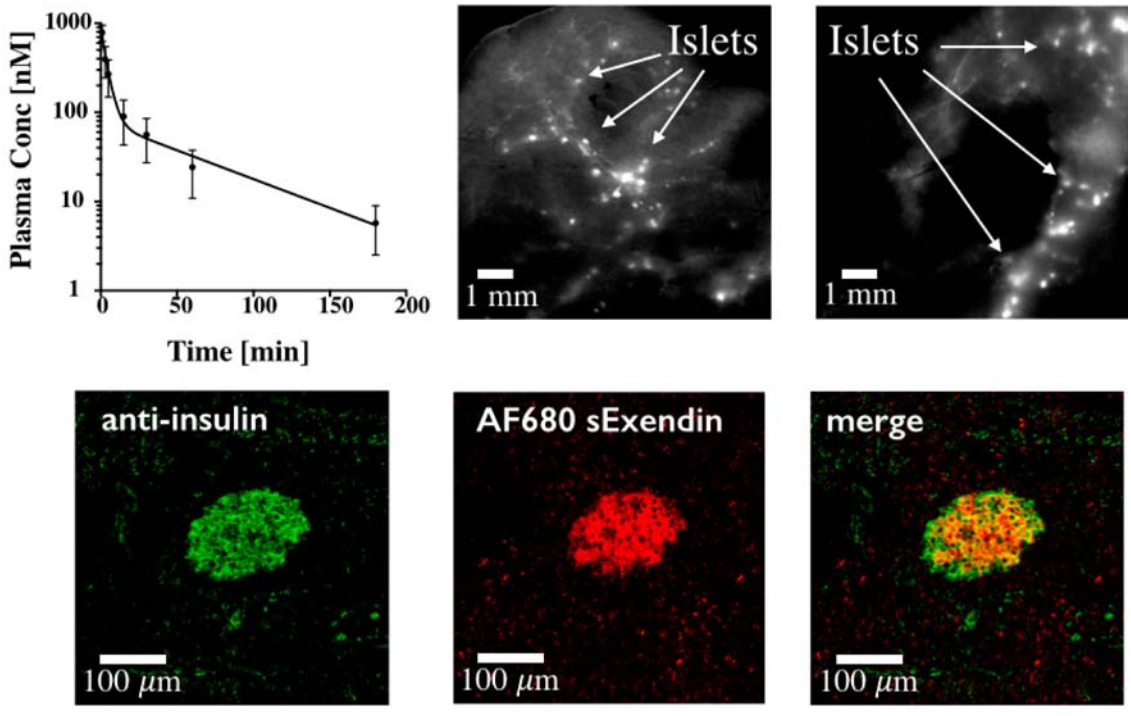

Figure 6. Stabilized fluorescent exendin clears rapidly from the plasma (top left) and efficiently targets islets, providing high tissue contrast (top middle). Beta cells form ~1 to 2% of the pancreas and are located in 100−300 μm islets of Langerhans that are labeled intensely by the fluorescent peptides (arrows). K12C labeled fluorescent exendin is shown for comparison (top right). Histology slide of pancreas showing *ex vivo* anti-insulin staining of islets (left), *in vivo* delivered AF680 sExendin (middle), and merge (right).

DOI: 10.1021/bc500584t
Bioconjugate Chem. 2015, 26, 329−337

analyzed the protease stability, helicity, and binding affinity of several helix stabilized derivatives.

For the linker design, propargyl bromide was used to react with the *N*-Boc-2,2′-(ethylenedioxy)diethylamine spacer for optimal cross-linker length. Previous reports of *i*, *i* + 7 linkers indicated that a 13-atom linker stabilizes an α-helix conformation.[8] Linker design was critical to avoid the stabilization of other types of helices[36] and the instability of longer linkers.[37] The facile incorporation of azidohomoalanine, either by synthetic techniques (SPPS) or biological systems,[38] makes this cross-linking chemistry advantageous for synthesizing stabilized helices. The 7-carbon span of the dialkyne generates a 13-atom cross-link for efficient stabilization of an α helix.

Stabilization of α helices reduces solvent interaction of the hydrophilic backbone and reportedly increases cell permeability for some peptides.[6,39] While membrane permeability is desirable for intracellular targets, this would increase the background signal of an imaging agent. A diethylene glycol spacer was placed between the amine functional handle and the dialkyne to impart additional hydrophilicity to the linker. Although the fluorescent dyes used in this work are charged and hydrophilic, the linker could aid in radiolabeling applications where the tag may be more lipophilic.[21]

As a model system for testing the dual-purpose linker, we chose exendin and GLP-1 peptides. We and others[19−21,23,25,30,33] have used exendin and stabilized GLP-1[22] for imaging beta cells and increasing therapeutic efficacy, and the peptides are well-characterized. Several GLP-1R agonists are in the clinic for treating type 2 diabetes,[40] and the crystal structures of both peptides bound to their target have been published.

The stabilized peptides were synthesized with moderate yield (9−63%) with the expected molecular weight shown by MALDI-TOF. Despite the homobifunctional cross-linking chemistry, little to no oligomerization was detected. This is likely due to templating effects from the peptide backbone[11] and is in agreement with the higher yield for the more helical exendin-4 peptide compared to that of GLP-1. An additional linker, 1,4-diethynylbenzene, was tested to see if the increased strain from a more rigid, linear cross-linking agent would stabilize or destabilize the helix. However, yields of this reaction were extremely low, likely due to inefficient cross-linking (data not shown). The stabilized helices showed up to a 14-fold increase in trypsin protease stability. For exendin, the three predicted cleavage sites include one site within the cross-link, one just outside the cross-link, and a third several residues away. Proteases recognize an extended β-strand conformation, so either direct steric hindrance by non-natural amino acids and cross-links or a helical conformation can prevent degradation.[41] A combination of these factors likely contributes to the lack of protease digestion in our system.

Unexpectedly, double mutant GLP-1 had significantly increased protease stability. CD measurements indicated that the azidohomoalanine substitutions did not result in high helicity. One of the non-natural amino acids is located adjacent to a lysine cleavage site, potentially slowing the rate of proteolysis. However, LC-MS data indicated that this site was still cleaved (data not shown). While no aggregation was detected at lower concentrations during experiments, the substitution of a glutamic acid residue for azidohomoalanine reduced the charge of the peptide, and aggregation of double mutant GLP-1 at high concentrations during synthesis and protease digestion could have contributed to the low GLP-1 stabilization reaction yields and high protease stability. The data also did not fit an exponential decay very well, indicating that aggregation may play a role in its protease resistance. However, mutant GLP-1 protease resistance could be an example where the sequence mutations impart unique properties independent of the linker.[16] Notably, the linker was required for the large increase in exendin protease resistance.

Despite the larger cross-linking label, the K_d for AF680 sExendin only increased by 0.9 nM compared to double mutant exendin. Locating the linker opposite the binding interface and including a hydrophilic spacer allowed the peptide to maintain high binding affinity in addition to increased protease stability. The other cross-linking agents maintained high affinity of the exendin to GLP-1R but did not increase in affinity. This is likely due to the high helicity of the peptide even without a stabilizing side chain cross-link. To corroborate this argument, a three-state thermodynamic model of binding for helical peptides (Supporting Information) was used to show a negligible predicted increase in the binding affinity (0.42−0.53 nM) for exendin. The larger increase in helicity for GLP-1 derivatives results in a small but significant predicted increase in binding affinity ($K_d \sim 1.5$ nM) in the absence of steric effects and changes in the enthalpy of binding. Larger decreases in K_d are predicted for lower affinity peptides (Supporting Information).

The trade-off between a more rigid α helix (lowering the entropic penalty but reducing the enthalpy of binding) and a more flexible linker has been established for stabilized helices.[8] The stabilized GLP-1 peptides demonstrated a small but statistically significant increase in affinity and a large increase in helicity, consistent with the thermodynamic model. GLP-1 is disordered in solution, so stabilizing the α helix increases the affinity by lowering the entropic penalty upon binding. In principle, locking the GLP-1 peptide in a straight α helix could reduce affinity by removing the kink present in the crystal structure, and this level of detail is not captured in the simple three-state model. For GLP-1 however, it appears that the *i*, *i* + 7 cross-link is flexible enough to allow for high-affinity interactions or, at the very least, the reduction in the entropic penalty dominates the free energy of binding.

Comparing the more rigid 1,3-diethynylbenzene cross-linker versus the propargyl ether, it appears the latter has more helix-inducing propensity in these two peptides. While both linkers increased the protease stability and helicity of exendin and GLP-1, along with the affinity of GLP-1, the propargyl ether did so to a larger extent in each case. The additional flexibility likely makes the α helix more energetically favorable, thereby increasing protease stability, affinity, and helicity.

The stabilized fluorescent peptide maintained efficient targeting of beta cells *in vivo*. The rapid clearance from the plasma is beneficial for lowering background fluorescence but could potentially reduce targeting if insufficient amounts reach the beta cells. For tumors, an analysis of molecular weight versus targeting efficiency concluded that for small targeting agents the lower the molecular weight, the more efficient the uptake, provided that high affinity is maintained.[3] Low molecular weight agents were all filtered rapidly by the kidneys, but the smaller agents extravasated into the tumor more quickly. This has also driven protein engineers to find smaller scaffolds for rapid targeting.[42−44] It remains to be seen whether the same quantitative conclusions apply to the pancreas. Intravital microscopy experiments of exendin show rapid uptake in islets within several minutes after injection.[33] Islets

DOI: 10.1021/bc500584t
Bioconjugate Chem. 2015, 26, 329−337

are highly vascularized (500 cm^2/cm^3 blood vessel surface area to volume[21]) with fenestrated endothelium, which appears to allow efficient access to the target cells even over short circulation times.

We anticipate this dual-purpose linker will have applications with other peptides in imaging and therapeutic development. Recently, Lau et al. used a poly-arginine conjugated 1,3-diethynylbenzene cross-linker to increase cellular uptake of a p53 α helix.[45] In their MDM2 targeting peptide, they found a similar trend in which a more flexible aliphatic dialkyne produced better stabilization than a more rigid 1,3-diethynylbenzene.[46] This is analogous to our findings where flexible propargyl ether resulted in more efficient binding and helicity than 1,3-diethynylbenzene. Importantly, the propargyl ether and fluorescent linker maintain hydrophilicity for this extracellular target compared to that of intracellular MDM2-targeting peptides. The ability to both stabilize the α helix and impart additional functionality through the tertiary amine in our linker minimizes the impact of adding multiple sterically bulky groups. Successful α-helix stabilization in both the GLP-1R targeting peptides and MDM2 peptides provides evidence that this method may work as a general strategy. As seen with lactam bridges and hydrocarbon stapling, results can be sequence-dependent, and individual cases need to be tested.[16,18] Nevertheless, these functional linkers may have applications in several stabilized α-helix applications including imaging agents, drug design, surface modification, and affinity separations.[47,48]

In conclusion, we have reported a novel dual-purpose linker that is capable of labeling GLP-1 receptor ligands with an imaging agent modality, stabilizing the α-helix structure and increasing protease stability while having minimal impact or an improvement on binding affinity.

EXPERIMENTAL PROCEDURES

Materials. Double mutant exendin-4 (HGEGTFTSDLSK-QXEEEAVRXFIEWLKNGGPSSGAPPPS), double mutant GLP-1 (7−36, HAEGTFTSDVSSYXEGQAAKXF-IAWLVKGR), and single mutant exendin-4 (HGEGTFTSDLS-KQXEEEAVRLFIEWLKNGGPSSGAPPPS), where X is the non-natural amino acid AHA, were purchased from Innopep (San Diego, CA). Fluorochromes AF647 alkyne and AF680 *N*-hydroxysuccinimidyl (NHS) ester were purchased from Life Technologies (Carlsbad, CA). *N*-Boc-2,2′-(ethylenedioxy)-diethylamine, rabbit anti-insulin, and goat anti-rabbit IgG FITC antibodies were purchased from Santa Cruz Biotechnology (Dallas, TX). All other reagents, unless specified, were purchased from Sigma-Aldrich (Milwaukee, WI) and were used as received. Reverse-phase high-performance liquid chromatography (RP-HPLC) was performed on a Shimadzu LC unit using analytical and preparative reversed-phase Phenomenex Luna C18(2) columns. MALDI-MS spectra were collected using a Bruker Autoflex mass spectrometer, and ESI-MS analysis was performed on an Agilent Q-TOF 1200 series. NMR spectra were collected using a Varian MR400 spectrometer. Fluorescence microscopy images were collected using an Olympus FV 1200 confocal microscope.

Preparation of (1). *N*-Boc-2,2′-(ethylenedioxy)-diethylamine (805 μmol) was added to diisopropylethylamine (2.40 mmol) in 3.8 mL of MeCN. Propargyl bromide in toluene was added dropwise (2.62 mmol). The reaction mixture was stirred overnight at room temperature before being concentrated under reduced pressure and then subjected to flash chromatography (80:7:1 $CHCl_3$/MeOH/NH_4OH). The desired fraction was concentrated, deprotected using 50% trifluoroacetic acid in dichloromethane, and purified using preparative RP-HPLC using a linear gradient of MeCN in H_2O to yield **1** (475 μmol, 59%). ^{1}H NMR (400 MHz, CD_3OD): δ 3.89 (4H, d), 3.77 (2H, t), 3.73 (2H, t), 3.70 (4H, s), 3.18 (2H, t), 3.15 (2H, t), 3.04 (2H, t). ^{13}C NMR (400 MHz, CD_3OD): δ 76.8, 74.6, 69.9, 69.8, 66.5, 51.9, 42.2, 39.2. HRMS: m/z calcd for $C_{12}H_{20}N_2O_2$, 225.1603; found, 225.1600.

Preparation of (2). AF680 NHS ester (1 μmol in DMSO) was added to an aqueous solution containing **1** (10 μmol) buffered with 7.5% sodium bicarbonate. The reaction was stirred at room temperature for 30 min followed by purification on preparative RP-HPLC (12 mL/min; A: 0.1% trifluoroacetic acid in water, B: 0.1% trifluoroacetic acid in acetonitrile; 20% B 0.1−3 min, 20−40% B 3−11 min) to give **2**: t_R = 10.2 min. MALDI-TOF: m/z calcd, 1063.11; found, 1064.38. All MALDI-TOF and ESI-mass spectrometry data were collected at the University of Michigan Department of Chemistry's Core Facility.

Preparation of Stabilized Peptides. Propargyl ether (0.3 μmol), 1,3 diethynylbenzene (0.3 μmol), **2** (0.3 μmol), or AF647 alkyne (0.3 μmol) was first added to 200 μL of 1:1 water/*tert*-butanol, followed by Cu-TBTA (30 nmol) and sodium ascorbate (0.3 μmol). Lastly, double mutant peptide (0.3 μmol) was added, and the solution was gently stirred at room temperature for 12 h followed by purification on preparative RP-HPLC (propargyl ether stabilized exendin (PropE sExendin) and 1,3-diethynylbenzene stabilized exendin (DEB sExendin): 28% B 0.1−7 min, 28−70% B 7−23 min (PropE sExendin: 97% purity; DEB sExendin: 98% purity); AF680 linker stabilized exendin (AF680 sExendin), AF680 linker stabilized GLP-1 (AF680 sGLP-1), AF647 labeled exendin: 25% B 0.1−7 min, 25−70% B 7−20 min (AF680 sExendin: 92% purity; AF680 sGLP-1: 89% purity; AF647 exendin: 94% purity); propargyl ether stabilized GLP-1 (PropE sGLP-1): 37% B 0.1−7 min (PropE sGLP-1:93% purity); 1,3-diethynylbenzene stabilized GLP-1 (DEB sGLP-1): 23−38% B 0.1−12 min, 38−50% B 12−20 min (DEB sGLP-1:92% purity)) at a flow rate of 12 mL/min. MALDI-TOF: PropE Exendin: m/z calcd, 4288; found, 4288; DEB sExendin: m/z calcd, 4320; found, 4319; AF680 sExendin: m/z calcd, 5257; found, 5258; AF680 sGLP-1: m/z calcd, 4370; found, 4372; AF647 sExendin: m/z calcd, MW of dye unpublished; found, 4859; PropE sGLP-1: m/z calcd, 3401; found, 3400; DEB sGLP-1: m/z calcd, 3433; found, 3435. For quantifying peptide concentrations to determine yield and circular dichroism measurements, amino acid analysis was carried out by the University of Michigan Proteomics and Peptide Synthesis Core.

Cell Culture. NIT-1 cells, a GLP-1R positive mouse beta cell line, were generously provided by Dr. Ralph Weissleder's laboratory and used for receptor binding studies. Cells were grown in F12K containing 10% (v/v) heat-inactivated FBS, 50 U/mL penicillin, 50 μg/mL streptomycin, and 1.5 g/L sodium bicarbonate. The passage number for NIT-1 cells used in affinity measurements for all peptides was between 4 and 16

***In Vitro* Receptor Binding Assay.** NIT-1 cells were grown for 48 h before being harvested with trypsin-EDTA. The cells were then washed with PBS, centrifuged, and resuspended in PBS with 1.0% BSA. Cells were aliquoted and suspended in binding buffer containing stabilized GLP-1 or exendin on ice (0.05−250 nM). After 3 h, cells were centrifuged and washed (for fluorescent constructs) or the buffer was replaced with a

DOI: 10.1021/bc500584t
Bioconjugate Chem. 2015, 26, 329−337

second binding buffer containing 20 nM of AF647 exendin. After 1 h, cells were washed with PBS with 1.0% BSA and immediately analyzed using an Attune Acoustic Focusing Cytometer (Applied Biosystems). Binding affinity curves and statistical analysis were carried out using Prism 6.0 software.

Animals. All animal experiments were conducted in compliance with the University of Michigan University Committee on Use and Care of Animals (UCUCA). For measuring plasma clearance, AF680 sExendin (1.2 nmol) or a validated K12C fluorescent exendin control peptide[21,33] was injected in the lateral tail vein of C57BL/6 mice (6 mice total). At predetermined time points (1, 3, 5, 15, 30, 60, 180 min), retro-orbital blood samples were collected. A LI-COR Odyssey CLx scanner (Lincoln, NE) was used to measure the fluorescence intensity for each sample, and the intensities were converted to concentration using a dilution series of AF680 sExendin in mouse plasma. After 3 h, the mice were sacrificed, and the pancreas was resected. Islets were visualized by a near-infrared scan on a LI-COR Odyssey CLx scanner.

Histology and Microscopy. Pancreata resected from C57BL/6 mice injected with AF680 sExendin were submerged in OCT and frozen in chilled 2-methylbutane. The organ was then sectioned into 6 μm slices, fixed with 4% paraformaldehyde for 10 min, and incubated overnight at 4 °C with a rabbit anti-insulin primary antibody (dilution 1:150 in PBS with 0.1% BSA supplemented with 1% goat serum), followed by a 30 min room temperature incubation with goat anti-rabbit IgG FITC secondary antibody (dilution 1:50 in PBS with 0.1% BSA).

Trypsin Digest. To assess the proteolytic resistance of stabilized peptides, both stapled and unstapled peptides (75 μM) were subject to a trypsin digest (500 ng/μL, pH 7.4, room temperature). Enzymatic digest was monitored at 254 nm using RP-HPLC to determine the degradation half-life.

Circular Dichroism (CD) Measurements. To quantify peptide secondary structure, CD spectra were collected on a Jasco-815 CD spectrometer with a 1 mm Hellma quartz cuvette at 23 °C. Five scans from 185 to 260 nm at 20 nm/min were averaged for peptide samples prepared in 5 mM potassium phosphate buffer, pH 7.0, at concentrations ranging between 5 and 20 μM, as determined by amino acid analysis. A scan containing only buffer/buffer with cross-linker was subtracted from sample scans. Helicity was calculated using mean residue ellipticity at 221 nm and maximum ellipticity as reported elsewhere.[27]

■ ASSOCIATED CONTENT

Supporting Information

Three-state thermodynamic model of stabilized alpha helix binding. This material is available free of charge via the Internet at http://pubs.acs.org.

■ AUTHOR INFORMATION

Corresponding Author

*E-mail: gthurber@umich.edu. Tel.: 734-764-8722.

Notes

The authors declare no competing financial interest.

■ ACKNOWLEDGMENTS

We thank the University of Michigan Biointerfaces Institute for assistance with CD measurements and Dr. Tim Scott's lab for assistance with gathering NMR data. Funding was provided by NIH grant 1K01DK093766 (G.M.T.).

■ REFERENCES

(1) Weissleder, R., and Pittet, M. J. (2008) Imaging in the era of molecular oncology. *Nature 452*, 580−9.
(2) Zhao, B. S., Schwartz, L. H., and Larson, S. M. (2009) Imaging surrogates of tumor response to therapy: anatomic and functional biomarkers. *J. Nucl. Med. 50*, 239−49.
(3) Schmidt, M. M., and Wittrup, K. D. (2009) A modeling analysis of the effects of molecular size and binding affinity on tumor targeting. *Mol. Cancer Ther. 8*, 2861.
(4) Akers, W. J., Zhang, Z. R., Berezin, M., Ye, Y. P., Agee, A., Guo, K., Fuhrhop, R. W., Wickline, S. A., Lanza, G. M., and Achilefu, S. (2010) Targeting of alpha(v)beta(3)-integrins expressed on tumor tissue and neovasculature using fluorescent small molecules and nanoparticles. *Nanomedicine 5*, 715−26.
(5) Kimura, R. H., Cheng, Z., Gambhir, S. S., and Cochran, J. R. (2009) Engineered knottin peptides: a new class of agents for imaging integrin expression in living subjects. *Cancer Res. 69*, 2435−42.
(6) Walensky, L. D., Kung, A. L., Escher, I., Malia, T. J., Barbuto, S., Wright, R. D., Wagner, G., Verdine, G. L., and Korsmeyer, S. J. (2004) Activation of apoptosis *in vivo* by a hydrocarbon-stapled BH3 helix. *Science 305*, 1466−70.
(7) Bird, G. H., Madani, N., Perry, A. F., Princiotto, A. M., Supko, J. G., He, X. Y., Gavathiotis, E., Sodroski, J. G., and Walensky, L. D. (2010) Hydrocarbon double-stapling remedies the proteolytic instability of a lengthy peptide therapeutic. *Proc. Natl. Acad. Sci. U.S.A. 107*, 14093−8.
(8) Sia, S. K., Carr, P. A., Cochran, A. G., Malashkevich, V. N., and Kim, P. S. (2002) Short constrained peptides that inhibit HIV-1 entry. *Proc. Natl. Acad. Sci. U.S.A. 99*, 14664−9.
(9) Schafmeister, C. E., Po, J., and Verdine, G. L. (2000) An all-hydrocarbon cross-linking system for enhancing the helicity and metabolic stability of peptides. *J. Am. Chem. Soc. 122*, 5891−2.
(10) Neumann, H., Wang, K. H., Davis, L., Garcia-Alai, M., and Chin, J. W. (2010) Encoding multiple unnatural amino acids via evolution of a quadruplet-decoding ribosome. *Nature 464*, 441−4.
(11) Torres, O., Yuksel, D., Bernardina, M., Kumar, K., and Bong, D. (2008) Peptide tertiary structure nucleation by side-chain crosslinking with metal complexation and double "click" cycloaddition. *ChemBioChem 9*, 1701−5.
(12) Yu, C. X., and Taylor, J. W. (1999) Synthesis and study of peptides with semirigid i and i+7 side-chain bridges designed for alpha-helix stabilization. *Bioorg. Med. Chem. 7*, 161−75.
(13) Galande, A. K., Bramlett, K. S., Trent, J. O., Burris, T. P., Wittliff, J. L., and Spatola, A. F. (2005) Potent inhibitors of LXXLL-based protein−protein interactions. *ChemBioChem 6*, 1991−8.
(14) Jackson, D. Y., King, D. S., Chmielewski, J., Singh, S., and Schultz, P. G. (1991) General approach to the synthesis of short alpha-helical peptides. *J. Am. Chem. Soc. 113*, 9391−2.
(15) Bird, G. H., Gavathiotis, E., LaBelle, J. L., Katz, S. G., and Walensky, L. D. (2014) Distinct BimBH3 (BimSAHB) stapled peptides for structural and cellular studies. *ACS Chem. Biol. 9*, 831−7.
(16) Okamoto, T., Segal, D., Zobel, K., Fedorova, A., Yang, H., Fairbrother, W. J., Huang, D. C., Smith, B. J., Deshayes, K., and Czabotar, P. E. (2014) Further insights into the effects of pre-organizing the BimBH3 helix. *ACS Chem. Biol. 9*, 838−9.
(17) Okamoto, T., Zobel, K., Fedorova, A., Quan, C., Yang, H., Fairbrother, W. J., Huang, D. C., Smith, B. J., Deshayes, K., and Czabotar, P. E. (2013) Stabilizing the pro-apoptotic BimBH3 helix (BimSAHB) does not necessarily enhance affinity or biological activity. *ACS Chem. Biol. 8*, 297−302.
(18) Giordanetto, F., Revell, J. D., Knerr, L., Hostettler, M., Paunovic, A., Priest, C., Janefeldt, A., and Gill, A. (2013) Stapled vasoactive intestinal peptide (VIP) derivatives improve VPAC2 agonism and glucose-dependent insulin secretion. *ACS Med. Chem. Lett. 4*, 1163−8.
(19) Reiner, T., Thurber, G., Gaglia, J., Vinegoni, C., Liew, C. W., Upadhyay, R., Kohler, R. H., Li, L., Kulkarni, R. N., Benoist, C., et al. (2011) Accurate measurement of pancreatic islet beta-cell mass using a second-generation fluorescent exendin-4 analog. *Proc. Natl. Acad. Sci. U.S.A. 108*, 12815−20.

DOI: 10.1021/bc500584t
Bioconjugate Chem. 2015, 26, 329−337

(20) Brand, C., Abdel-Atti, D., Zhang, Y., Carlin, S., Clardy, S. M., Keliher, E. J., Weber, W. A., Lewis, J. S., and Reiner, T. (2014) *In vivo* imaging of GLP-1R with a targeted bimodal PET/fluorescence imaging agent. *Bioconjugate Chem. 25*, 1323−30.
(21) Keliher, E. J., Reiner, T., Thurber, G. M., Upadhyay, R., and Weissleder, R. (2012) Efficient ^{18}F-labeling of synthetic exendin-4 analogues for imaging beta cells. *ChemistryOpen*, 177−83.
(22) Gao, H., Niu, G., Yang, M., Quan, Q., Ma, Y., Murage, E. N., Ahn, J.-M., Kiesewetter, D. O., and Chen, X. (2011) PET of insulinoma using ^{18}F-FBEM-EM3106B, a new GLP-1 analogue. *Mol. Pharmaceutics. 8*, 1775−82.
(23) Mikkola, K., Yim, C. B., Fagerholm, V., Ishizu, T., Elomaa, V. V., Rajander, J., Jurttila, J., Saanijoki, T., Tolvanen, T., Tirri, M., et al. (2014) ^{64}Cu- and ^{68}Ga-labelled [Nle^{14},Lys^{40}(Ahx-NODAGA)NH$_2$]-exendin-4 for pancreatic beta cell imaging in rats. *Mol. Imaging Biol. 16*, 255−63.
(24) Wicki, A., Wild, D., Storch, D., Seemayer, C., Gotthardt, M., Behe, M., Kneifel, S., Mihatsch, M. J., Reubi, J. C., Macke, H. R., et al. (2007) [Lys^{40}(Ahx-DTPA-^{111}In)NH$_2$]-exendin-4 is a highly efficient radiotherapeutic for glucagon-like peptide-1 receptor-targeted therapy for insulinoma. *Clin. Cancer Res. 13*, 3696−705.
(25) Wild, D., Wicki, A., Mansi, R., Behe, M., Keil, B., Bernhardt, P., Christofori, G., Ell, P. J., and Macke, H. R. (2010) Exendin-4-based radiopharmaceuticals for glucagonlike peptide-1 receptor PET/CT and SPECT/CT. *J. Nucl. Med. 51*, 1059−67.
(26) Underwood, C. R., Garibay, P., Knudsen, L. B., Hastrup, S., Peters, G. H., Rudolph, R., and Reedtz-Runge, S. (2010) Crystal structure of glucagon-like peptide-1 in complex with the extracellular domain of the glucagon-like peptide-1 receptor. *J. Biol. Chem. 285*, 723−30.
(27) Andersen, N. H., Brodsky, Y., Neidigh, J. W., and Prickett, K. S. (2002) Medium-dependence of the secondary structure of exendin-4 and glucagon-like-peptide-1. *Bioorg. Med. Chem. 10*, 79−85.
(28) Runge, S., Thogersen, H., Madsen, K., Lau, J., and Rudolph, R. (2008) Crystal structure of the ligand-bound glucagon-like peptide-1 receptor extracellular domain. *J. Biol. Chem. 283*, 11340−7.
(29) Adelhorst, K., Hedegaard, B. B., Knudsen, L. B., and Kirk, O. (1994) Structure−activity studies of glucagon-like peptide-1. *J. Biol. Chem. 269*, 6275−8.
(30) Clardy, S. M., Keliher, E. J., Mohan, J. F., Sebas, M., Benoist, C., Mathis, D., and Weissleder, R. (2014) Fluorescent exendin-4 derivatives for pancreatic beta-cell analysis. *Bioconjugate Chem. 25*, 171−7.
(31) Parker, J. C., Andrews, K. M., Rescek, D. M., Massefski, W., Jr., Andrews, G. C., Contillo, L. G., Stevenson, R. W., Singleton, D. H., and Suleske, R. T. (1998) Structure−function analysis of a series of glucagon-like peptide-1 analogs. *J. Pept. Res. 52*, 398−409.
(32) Martin, S. F. (2007) Preorganization in biological systems: are conformational constraints worth the energy? *Pure Appl. Chem. 79*, 193−200.
(33) Reiner, T., Kohler, R. H., Liew, C. W., Hill, J. A., Gaglia, J., Kulkarni, R. N., and Weissleder, R. (2010) Near-infrared fluorescent probe for imaging of pancreatic beta cells. *Bioconjugate Chem. 21*, 1362−8.
(34) James, M. L., and Gambhir, S. S. (2012) A molecular imaging primer: modalities, imaging agents, and applications. *Physiol. Rev. 92*, 897−965.
(35) Lee, S., Xie, J., and Chen, X. (2010) Peptide-based probes for targeted molecular imaging. *Biochemistry 49*, 1364−76.
(36) Jacobsen, O., Maekawa, H., Ge, N. H., Gorbitz, C. H., Rongved, P., Ottersen, O. P., Amiry-Moghaddam, M., and Klaveness, J. (2011) Stapling of a 3_{10}-helix with click chemistry. *J. Org. Chem. 76*, 1228−38.
(37) Scrima, M., Le Chevalier-Isaad, A., Rovero, P., Papini, A. M., Chorev, M., and D'Ursi, A. M. (2010) Cu-I-catalyzed azide-alkyne intramolecular *i*-to-(*i*+4) side-chain-to-side-chain cyclization promotes the formation of helix-like secondary structures. *Eur. J. Org. Chem.*, 446−57.
(38) Johnson, J. A., Lu, Y. Y., Van Deventer, J. A., and Tirrell, D. A. (2010) Residue-specific incorporation of non-canonical amino acids into proteins: recent developments and applications. *Curr. Opin. Chem. Biol. 14*, 774−80.
(39) Muppidi, A., Wang, Z. Y., Li, X. L., Chen, J. D., and Lin, Q. (2011) Achieving cell penetration with distance-matching cysteine cross-linkers: a facile route to cell-permeable peptide dual inhibitors of Mdm2/Mdmx. *Chem. Commun. 47*, 9396−8.
(40) Ahren, B., and Schmitz, O. (2004) GLP-1 receptor agonists and DPP-4 inhibitors in the treatment of type 2 diabetes. *Horm. Metab. Res. 36*, 867−76.
(41) Tyndall, J. D., and Fairlie, D. P. (1999) Conformational homogeneity in molecular recognition by proteolytic enzymes. *J. Mol. Recognit. 12*, 363−70.
(42) Moore, S. J., Gephart, M. G. H., Bergen, J. M., Su, Y. R. S., Rayburn, H., Scott, M. P., and Cochran, J. R. (2013) Engineered knottin peptide enables noninvasive optical imaging of intracranial medulloblastoma. *Proc. Natl. Acad. Sci. U.S.A. 110*, 14598−603.
(43) Stern, L. A., Case, B. A., and Hackel, B. J. (2013) Alternative non-antibody protein scaffolds for molecular imaging of cancer. *Curr. Opin. Chem. Eng. 2*, 425−32.
(44) Goldstein, R., Sosabowski, J., Livanos, M., Leyton, J., Vigor, K., Bhavsar, G., Nagy-Davidescu, G., Rashid, M., Miranda, E., Yeung, J., et al. (2014) Development of the designed ankyrin repeat protein (DARPin) G3 for HER2 molecular imaging. *Eur. J. Nucl. Med. Mol. Imaging.*, DOI: 10.1007/s00259-014-2940-2.
(45) Lau, Y. H., de Andrade, P., Quah, S. T., Rossmann, M., Laraia, L., Skold, N., Sum, T. J., Rowling, P. J. E., Joseph, T. L., Verma, C., et al. (2014) Functionalised staple linkages for modulating the cellular activity of stapled peptides. *Chem. Sci. 5*, 1804−9.
(46) Lau, Y. H., de Andrade, P., McKenzie, G. J., Venkitaraman, A. R., and Spring, D. R. (2014) Linear aliphatic dialkynes as alternative linkers for double-click stapling of p53-derived peptides. *ChemBioChem*, 2680−3.
(47) Li, H., Aneja, R., and Chaiken, I. (2013) Click chemistry in peptide-based drug design. *Molecules 18*, 9797−817.
(48) White, C. J., and Yudin, A. K. (2011) Contemporary strategies for peptide macrocyclization. *Nat. Chem. 3*, 509−24.

DOI: 10.1021/bc500584t
Bioconjugate Chem. 2015, 26, 329−337